Hydrology Research

British Hydrological Society

IWA PUBLISHING

Hydrology Research Vol 54 No 2, 136 doi: 10.2166/nh.2023.026

Baseflow index characterization in typical temperate to dry climates: conceptual analysis and simulation experiment to assess the relative role of climate forcing features and catchment geological settings

Antonia Longobardi[a,*] and Paolo Villani[a,b]

[a] Department of Civil Engineering, University of Salerno, Via Ponte Don Melillo, Fisciano, SA 84084, Italy
[b] CUGRI Consorzio Inter-Universitario per la previsione e prevenzione dei Grandi Rischi, Via Ponte Don Melillo, Fisciano, SA 84084, Italy
*Corresponding author. E-mail: alongobardi@unisa.it

AL, 0000-0002-1575-0782

ABSTRACT

Low-flow hydrological features are crucial for efficient development and integrated water resources management. Among others, the Base-Flow Index 'BFI' is one of the most important low-flow indices. Many studies have demonstrated that it is related to several topographic parameters, climate, vegetation and soil types and to catchment geology. With the aim to enhance the knowledge about the climate and catchment properties' relative control on the 'BFI', an approach consisting of an empirical analysis, applied to a large area located in Southern Italy, characterized by a typical Mediterranean environment, is followed by a simulation experiment, considering climate settings, at the pan-European scale, typical of temperate to dry climate regimes. Main findings have revealed that (i) the correlation structure between the 'BFI' and the precipitation volume, at the annual scale, is affected by both climate variability and catchment properties; (ii) the 'BFI' variability is strongly conditioned by climate intra- and inter-annual variability; (iii) the major role is, however, assigned to the geological catchment features, with poorly and well-drained catchments behaving differently in response to similar climate forcing variability.

Key words: BFI, precipitation inter-annual variability, precipitation intra-annual variability, regional analysis

HIGHLIGHTS

- The role of climate control on the baseflow index (BFI) is explored.
- Typical temperate to dry climatic areas are investigated.
- Climate variability affects the correlation between the BFI and rainfall.
- BFI variability is strongly conditioned by climate intra and inter-annual variability.

1. INTRODUCTION

Low flow is an integral seasonal component of the hydrological regime whose quantification is crucial for efficient development and integrated water resources management and also for maintenance of quantity and quality of water for irrigation, recreation, and wildlife conservation. Considered as, in a general sense, the actual flows occurring in a river during the dry season of the year, low flows can be summarized by a number of measures or indices and among them, the BaseFlow Index, 'BFI', can be mentioned as one of the most widely used statistics. The 'BFI' is defined as the ratio between the baseflow and the total streamflow volume and many studies have demonstrated that it is related to several climatic and catchment properties (Mehaiguene *et al.* 2012; Ahiablame *et al.* 2013; Yao *et al.* 2021).

Climatic measures have been soundly and successfully used as independent variables in statistical multiple linear regression models for regional low-flow prediction. Frequently, only average climate measures, such as mean annual precipitation (MAP) and mean annual potential evapotranspiration (MAPE), have been considered (Van Dijk 2009; Beck *et al.* 2013; Lyu *et al.* 2022). But rainfall variability can directly or even indirectly affect many processes occurring within the hydrosphere. In the recent literature, scientific contributions commented on the importance of more specific climatic features to be accounted for better understanding, especially in particular climatic regions. With regard to the 'BFI', Schneider *et al.*

(2007), in a European context, argued that soil classes are in fact sufficient to predict the 'BFI' but that the variability explained through geological properties tends to decrease from Northern to Southern Europe, probably because factors such as climate and its variability, which are not obviously used to differentiate soil classes, have a greater influence, especially in specific areas. Wu *et al.* (2019) found that climate variability was the main factor altering the 'BFI' in 11 catchments located within the semi-arid Loess Plateau and the climate effect can be even larger than the human activities effect. In arid and semi-arid environments, the baseflow generation is limited by vaporization and the aridity index is the primary determinant of baseflow (Gnann *et al.* 2019). Hellwig *et al.* (2021) showed how across Germany, in a temperate climate setting, climates with higher total annual recharge, but more frequent or severe summer droughts, groundwater droughts might become less severe while the baseflow drought hazard becomes more severe.

Catchment properties and more specifically hydrogeological properties play an undeniable role in baseflow generation with specificities that are hardly recognized on a large scale. Using the hydrological regime characterization, considering the distinction between intermittent and persistent river regimes, Botter *et al.* (2013) found in a study across the United States, that erratic systems are more resilient to climate fluctuation, where perhaps catchment control is dominant. In a similar context, at the pan-European scale, Longobardi & Van loon (2018) found that systems located in the transition zone between poorly and well-drained catchments are the most vulnerable to climate fluctuation, where perhaps catchment control is dominant.

Despite a very large body of literature, there is still no general theory able to interpret the relative role of climate and catchment controls on baseflow generation (Gnann *et al.* 2019). Understanding baseflow droughts in order to achieve sustainable groundwater management, especially in light of climate change responsiveness, is crucial, therefore it is important to contribute empirical and modelling analyses to the knowledge of the scientific community in exploring 'BFI' controls.

In this research paper, an initial empirical analysis, concerning a wide region located in Southern Italy, featured by a typical Mediterranean climate, is followed by a hydrological simulation experiment concerning a broad range of climate conditions at the pan-European scale, from temperate to dry climate areas. Beyond climate properties, also a wide range of catchment geological settings were considered, from poorly to well-drained system. Both observed (empirical analysis) and synthetic (simulation experiment) streamflow time series were filtered to derive the 'BFI' and the 'BFI' variability index. Specifically, the presented research aimed at:

- Understand the role of climate properties on 'BFI' and 'BFI' variability assessment and in particular understand the specific importance of climate average and variability indices on 'BFI' assessment.
- Understand which is the relative role of climate and catchment attributes, for a wide range of hydrological system conditions.

The findings of the research will help in shading light on the identification of the hydrological system which are most impacted by climate properties as they will represent the system that will be most impacted by climate change and for which mitigation strategies are needed to preserve freshwater resources.

2. STUDY AREA AND DATA

The case study is a wide region of about 25,000 km^2, located within the Campania region, Southern Italy. Hydrologic data consist of daily streamflow time series for 28 stream gauge sites, and their locations are shown in Figure 1. For a comprehensive description of the database, refer to Longobardi & Villani (2008), where the assessment of the 'BFI', the permeability P index, assumed to represent the catchment geological settings, and the relevant empirical relationship is provided. P is computed starting from the map of hydro-geomorphological classes represented in Figure 1, which combines the information about geology, land use and catchment slope. It is defined as the ratio between the catchment area falling into categories A and B and the total catchment area. Class A corresponds to pervious and bare geological complexes whereas class B corresponds to pervious and forested geological complexes. The 'BFI' ranges from 25 to 87%, and the catchment permeability index P ranges from 3 to 97%, providing indications for a region featured by very heterogeneous geological settings.

Climate data for the studied region are provided in Longobardi & Boulariah (2022). MAP, ranges from 859 to 1,633 mm/year, and the Thornthwaite MAPE, ranges from 576 to 837 mm/year, describing a typical subhumid climate, close to the subarid limit. To account for inter-annual and intra-annual precipitation variability, respectively, the coefficient of variation of the annual precipitation (Cv(MAP)) and the Precipitation Concentration Index (PCI) were accounted for. On a climate base, the studied region falls into what is called the dry-summer subtropical climate, also known as the Mediterranean climate. Both Cv(MAP) and the PCI showed almost constant values over the studied region, providing indications for a seasonal climate

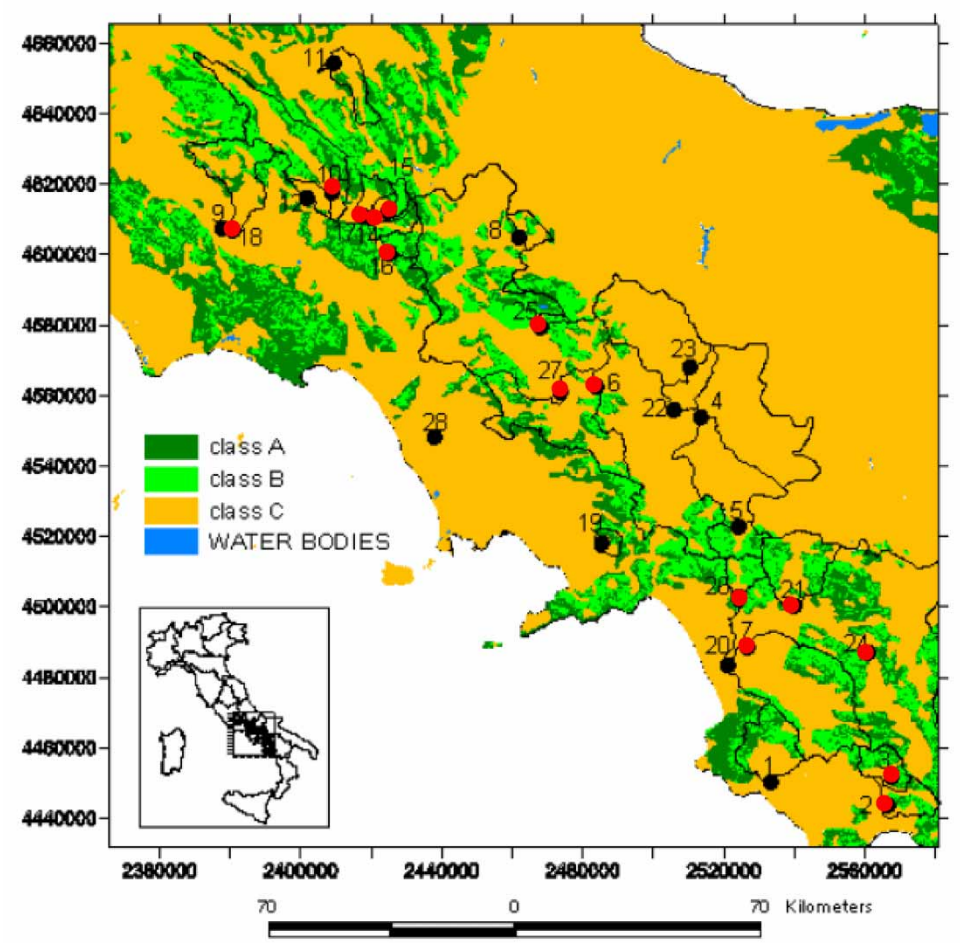

Figure 1 | Map of hydro-geomorphological units for the Campania region (Class A = pervious and bare; Class B = pervious and forested; Class C = impervious, Longobardi & Villani 2008). Catchment locations are provided by circles corresponding to catchment outlets. Black circles correspond to group 1 in Figure 2. Red circles correspond to group 2 in Figure 3. Please refer to the online version of this paper to see this figure in colour: http://dx.doi.org/10.2166/nh.2023.026.

regime with moderate inter-annual variability and a substantial climate homogeneity condition (Longobardi & Boulariah 2022).

Geological influence on baseflow was found to be dominant within the studied area (Longobardi & Villani 2008; Longobardi & Villani 2013). According to the mentioned studies, for the study area, it was possible to predict the 'BFI' on the basis of the computation of a permeability index P, with the use of a simple univariate regression model, explaining about 70% of the variance and the mean square error of about 10%. The simple univariate model generally overestimated the 'BFI' for small P-values ($P < 40\%$), whereas for medium and large P, the model over- or under-predicted 'BFI' with no specific pattern.

3. METHODS

3.1. Empirical analysis

Provided the described importance of the geological settings on the 'BFI' prediction within the study area, the current research was aimed, furthermore, at the study of the role of climate features on the baseflow component. In the first step, this was investigated by the use of an empirical framework, based on the calibration of simple and multiple regression models, relating the 'BFI' to climate indices such as MAP, MAPE, Cv(MAP) coefficient of variation of the annual precipitation and PCI, beyond the catchment permeability index (P). The goodness-of-fit was measured in terms of mean squared

error (mse), correlation coefficient (r^2) and jack-knife errors. To improve the interpretative performance of the regression approach, the *k*-means algorithm was applied to the investigated catchments in order to group them on the basis of relevant climate indices (MAP and MAPE). The weak climate variability of the study area dampened the relevant findings about climate control on the 'BFI'. For this reason, a simulation approach was set up to explore a broader range of climate conditions.

3.2. Climate forcing

A methodology for daily synthetic rainfall time series generation was identified. Gridded rainfall monthly scale data from the EU F6 WATCH project (Harding *et al.* 2011) were analyzed, for about 210 grid points, in order to cover a broad range of climate conditions, at the pan-European scale, from the temperate to the dry climate properties. In particular, data from one North–South transect and four West–East transects, as illustrated in Figure 2, were considered.

Monthly rainfall data were characterized in terms of MAP, PCI and Cv(MAP). The effectiveness of the EU F6 WATCH project data at the pan-European scale was given in Longobardi & Van Loon (2018).

To scale from monthly data to daily scale data, rainfall data were furthermore described as a sequence of instantaneous rainfall events, each carrying a random amount of water, that is a compound Poisson process (Daly & Porporato 2006). Rainfall events occurrence was modelled as a series of point events, drawn from a Poisson distribution with parameter ν, and the amount of rainfall, for each event, was drawn from an exponential distribution with parameter λ. Parameters ν and λ were described on a monthly basis. The corresponding probability density function refers to the Bessel distribution (Benjamin & Cornell 1970):

$$P[I=0]=e^{-\nu} \quad for\, I=0 \tag{1}$$

$$f_I(I)=e^{-\lambda I-\nu}\sqrt{\frac{\nu\lambda}{I}}\Im_1\left[2\sqrt{\lambda I\nu}\right] \quad for\, I>0 \tag{2}$$

where $\Im_1(x)$ is the modified order 1 Bessel function. Relations between the sample moments and the distribution parameters are:

$$\mu_I=\frac{\nu}{\lambda}=\nu\beta \quad \sigma_I^2=\frac{2\nu}{\lambda^2}=2\nu\beta^2 \quad cv_I=\frac{\sigma_I}{\mu_I}=\sqrt{\frac{2}{\nu}} \tag{3}$$

where μ, σ^2 and cv are, respectively, the precipitation mean, variance and monthly coefficient of variation and $\beta=1/\lambda$ is the average storm depth, in mm.

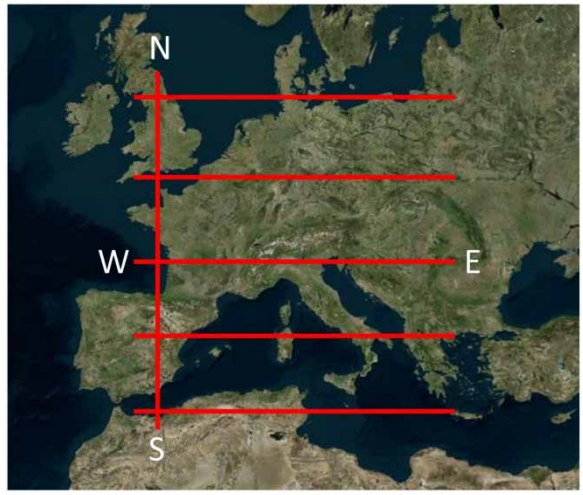

Figure 2 | Representation of the transects for which WATCH monthly precipitation data have been analyzed.

The v and β monthly patterns and values were derived for the 210 gridded point rainfall EU F6 WATCH data. A sub-set of 30 different v and β monthly patterns were selected, among the total estimations for the 210 gridded point data, to generate 30 synthetic daily rainfall time series over a long period (100 years), covering the pan-European temperate to dry climatic zones.

3.3. Simulation analysis

Generated synthetic daily rainfall time series were used as the input for a hydrological model in order to generate a large set of hydro-meteorological records, representative of the wide range of climate and geological properties aimed to be explored. The IHACRES (Jackeman *et al.* 1990) model has been selected in force of relevant previous applications involving the exploration of many issues, from climate and land cover change impact on the hydrological cycle to regional studies for ungauged basin prediction purposes and it was also recently applied to investigate the vulnerability of the 'BFI' to dry spell length in a pan-European scale study (Longobardi & Van Loon 2018). The IAHCRES model has six dynamic response parameters, namely '*f*' the temperature modulator factor, '*C*' the catchment storage index, 'τw' the catchment drying time constant, 'τs' the slow pathway time constant', 'τq' the quick pathway time constant, 'vs' the slow pathway proportional volume. The validation of the suitability of the IHACRES model to interpret the hydrological behaviour of the region under investigation was provided in Longobardi & Van Loon (2018) for a sub-set of the Italian catchments used in the current study. Geological properties were introduced in the simulation experiment through a conscious selection of dynamic catchment response model parameters. Since the analyses were focused on baseflow-related processes, the choice was oriented only on the assessment of the impact of two parameters, the slow pathway time constant τs and the proportional volume vs, tightly dependent on groundwater or aquifer percentage to total streamflow (Sefton & Howarth 1998).

Synthetic daily long-term total streamflow time series were processed and filtered to derive low-flow statistics. The IHACRES model provides a separation between the slow and fast pathways, but in order to consider a hydrograph filtering method that would have been independent of the hydrological catchment response simulation framework, reference was made to filtering techniques proposed in the current scientific literature. The SMT (Institute of Hydrology 1980) was selected as a simple smoothing and separation rule to separate the baseflow from the total streamflow hydrograph. Once baseflow time series were extracted from total streamflow, the following were evaluated: (i) the long-term 'BFI', as the ratio between the total baseflow volume and the total streamflow volume; (ii) an annual series of annual 'BFI', the ratio between annual baseflow and annual total streamflow, (iii) the mean and the standard deviation of the series at point (ii); (iv) the coefficient of variation of the 'BFI' Cv(BFI), as the ratio between the standard deviation and average value at point (iii).

4. RESULTS

4.1. Empirical analysis of the 'BFI' dependence on climate and geology indices

It was found that climate variables such as MAP, Cv(MAP), PCI and MAPE were only poorly related to the 'BFI'. The correlation coefficients of a simple regression model between 'BFI' and mentioned climate variables amounted respectively to 0.13, −0.01, 0.17, and −0.23. Their impact in the 'BFI' prediction was tentatively also included in a step-wise multiple regression approach. The *t*-test and *F*-test for Cv(MAP), PCI and MAPE regression coefficients showed *P*-values larger than the 5% significance level and they were excluded from the analysis. The multiple regression, based on P and MAP, had better performance indices compared to the simple regression method. The explained variance increases up to about 82%, the goodness-of-fit increase to a value of $r^2 = 0.77$ and the decreases to 7% (Table 1). Also the jack-knife errors, mean total true error (mt), mean apparent error (ma), as measures of goodness-of-fit, and mean expected excess error (me), as measures of model robustness, indicating a better performance.

To further improve the 'BFI' prediction, the k-means clustering algorithm was explored to use climate as a grouping rule rather than an independent variable in regression modelling (Laaha & Bloschl 2006). Two grouping rules were accounted for, one based on MAP values and the second based on MAP and MAPE, and a number of two clusters appeared optimal for each partition, in order to furthermore guarantee an adequate dimension of the samples to be analyzed. For each of the different resulting clustering and for each group, a simple regression model was fitted between P and the 'BFI' (Figure 2). The simple linear regression models, fitted on observed data for each group, satisfactorily described the variation of the catchment scale 'BFI' (Table 1). The explained variance was about 74–85%, depending on the group identification, however larger than the case of simple regression fitted on the whole dataset.

Both in the case of MAP and MAP + MAPE clustering (Figure 3), groups selection identified group 1 (grey circles) featured by MAP values below a threshold value of about 1,100 mm and MAPE values above a threshold value of about 700 mm

Table 1 | Regression model performances

Model	Groups	mse	r^2_{adj}	r² (obs-pre)	mt (%)	ma (%)	me (%)
Simple linear (P) (Longobardi & Villani 2008)	–	9.92	0.69	0.54	8.05	7.43	3.08
Multiple linear (P, MAP)	–	7.16	0.82	0.77	5.67	5.09	2.48
Simple linear (P) cluster based (MAP)	1	8.26	0.78	0.71	7.63	6.47	4.03
	2	9.22	0.74				
Simple linear (P) cluster based (MAP + MAPE)	1	9.16	0.74	0.76	7.28	5.70	4.53
	2	6.48	0.85				

Note: mse = mean squared error, r2adj = coefficient of determination adjusted for number of model parameters, r2 obs-pre = observed vs predicted scatter plot coefficient of determination, mt mean total, ma absolute and me expected jack-knife errors.

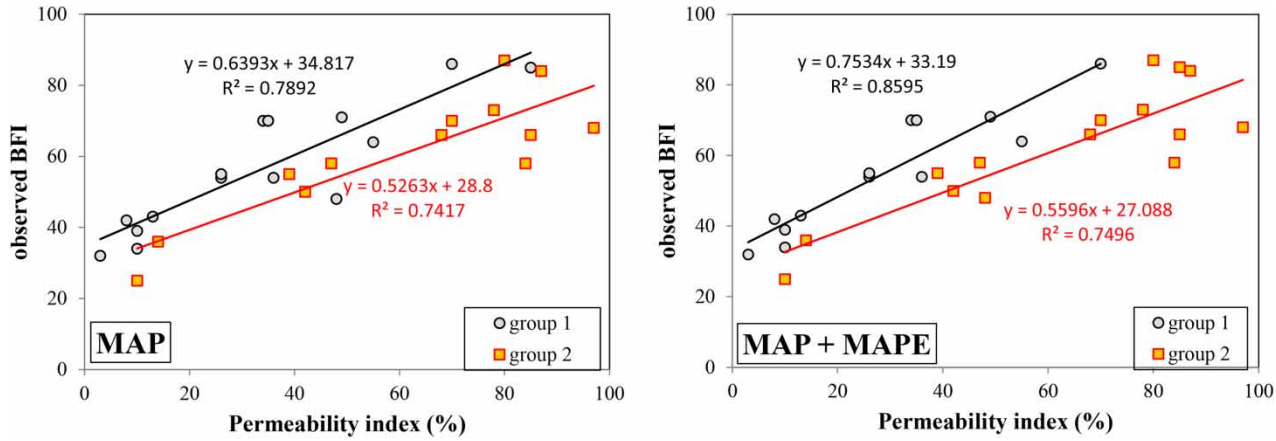

Figure 3 | A simple linear regression model between the 'BFI' and P, based on climate cluster. Please refer to the online version of this paper to see this figure in colour: http://dx.doi.org/10.2166/nh.2023.026.

(Table 2). The reverse holds in the case of group 2 (orange squares). The spatial location of group 1 and group 2 within the study region is represented in Figure 1.

In consideration of the regional annual average values of about 1,280 mm for precipitation and 690 mm for potential evapotranspiration, it could be underlined that group 1 corresponds to areas of the investigated region where the effective precipitation is low (low rainfall and high evapotranspiration). Additionally, catchments included in group 1 are characterized by a lower average permeability index P, regardless of the grouping rule (Table 2). Nevertheless, in each of the two grouping cases (Figure 2), the relative position of group 1 with respect to group 2, corresponds, for a given value of P, to a large 'BFI' for group 1.

Land cover is likely to contribute to specific effects highlighted in the case study. Forest cover is typically represented by the Mediterranean forest, which consists mainly of conifers, whose impact on the interception of rainfall may reach values up to

Table 2 | Average value for MAP, MAPE, P and FOR (percentage of forest cover), for each group identified by the two clustering partitioning methods

Methods	Groups	MAP (mm)	MAPE (mm)	P (%)	FOR (%)
MAP clustering partitioning	1	1,141	705	29	38
	2	1,447	673	58	51
MAP + MAPE clustering partitioning	1	1,119	712	33	33
	2	1,425	672	61	54

30% (Iovino *et al.* 2009). In the investigated area, the catchments belonging to group 1 (lower MAP values) have been found to be those with a moderate percentage of forest cover (Figure 4 and Table 2). This feature is also clear in Figure 1.

Instead, in group 2, characterized by the larger rainfall contribution and the smaller potential evapotranspirative loss (therefore larger effective rainfall), the fraction of wooded area is relevant and can be as high as about 90% (for a specific catchment) of the area of the basin (Figure 4). In these basins, therefore, the interception losses can be substantial, significantly reducing the effective rainfall volume and then the recharge to deep aquifers, potentially yielding smaller 'BFI' values, for an assigned level of permeability. In support of this thesis, experimental studies conducted in a dominant pine stands of a Mediterranean geographical contiguous area, have demonstrated that after thinning, a significant increase in groundwater flow has occurred, especially during spring and summer (Callegari *et al.* 2003).

4.2. Climate forcing settings characterization and rainfall generation

In order to generate daily scale rainfall data, which mimic given climate settings, the gridded monthly precipitation data from the EU F6 WATCH project (Harding *et al.* 2011) for about 210 grid point were analyzed. In particular, data from one North–South transect and four West–East transects, as illustrated in Figure 5, were considered.

At the pan-European scale, MAP, inter-annual variability Cv(MAP) (annual precipitation coefficient of variation) and intra-annual variability PCI indices appeared related to each other (Figure 5). Similar findings were also found for a specific region under investigation (Longobardi & Boulariah 2022) and at the global scale (Fatichi *et al.* 2012). A main trend exists with large values of PCI associated with large values of Cv(MAP). EU F6 WATCH data covered a large domain (Figure 6, middle plot,

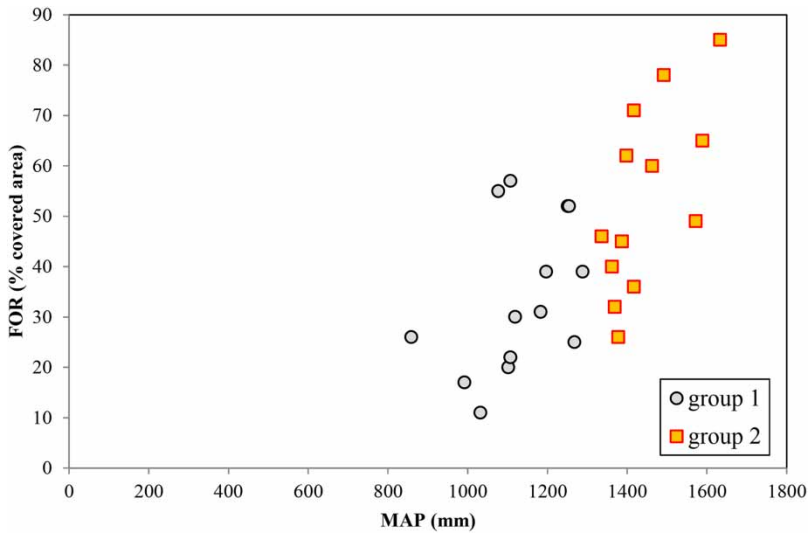

Figure 4 | MAP versus percentage of forest covered area (FOR) for the studied area. Group 1 and group 2 identification belongs to the MAP + MAPE clusters partitioning method.

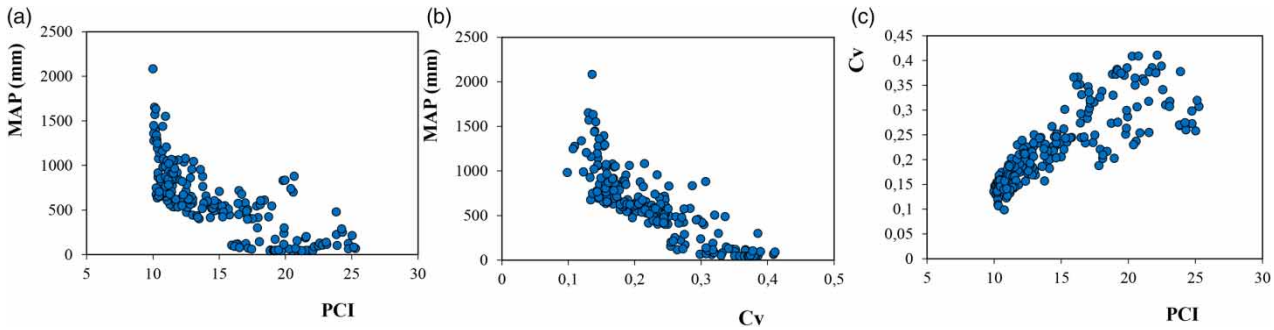

Figure 5 | Correlation between MAP, PCI, and Cv(MAP) for the analysed transects data.

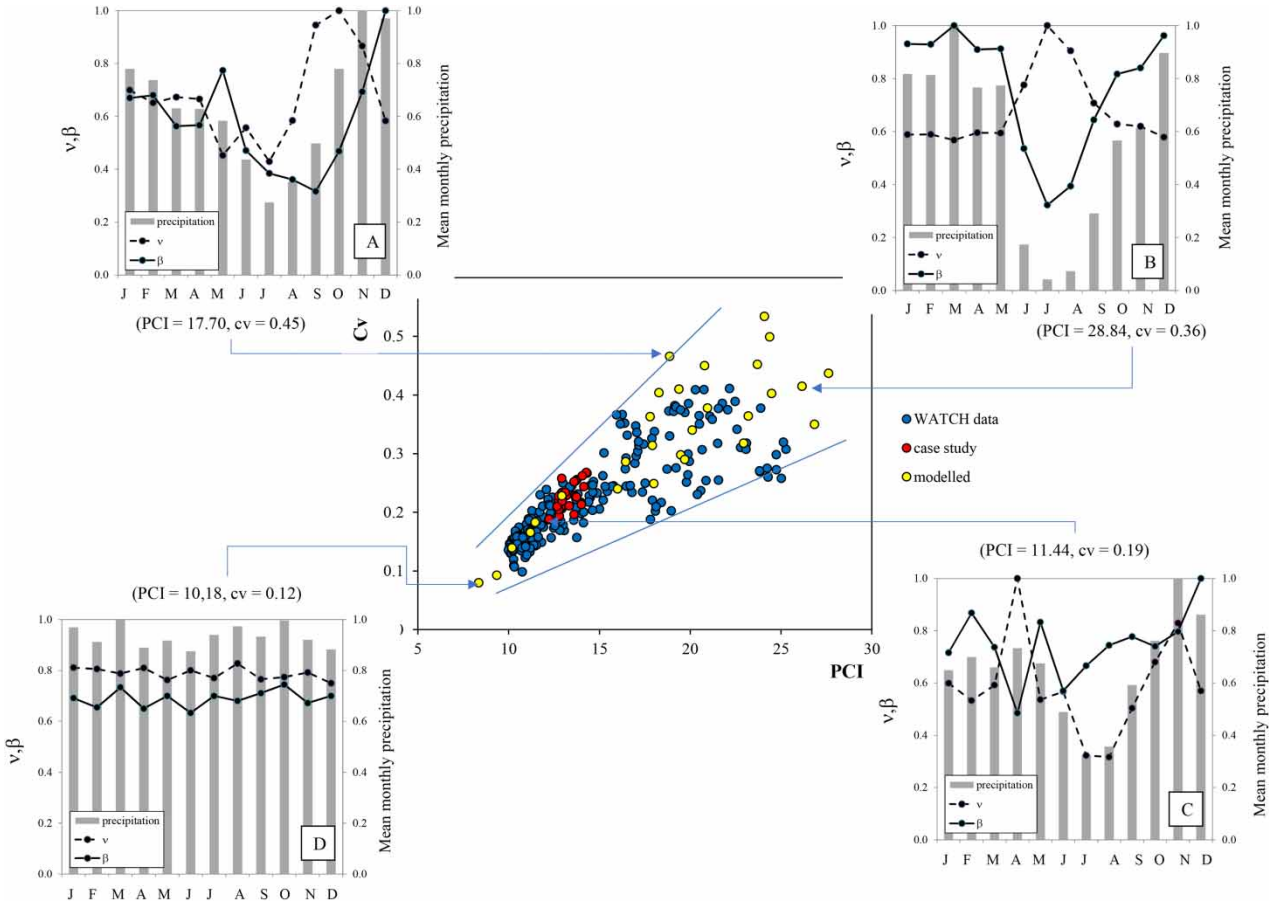

Figure 6 | PCI versus annual Cv(MAP) correlation for typical temperate to dry climate areas. In the middle, WATCH data (blue circles), case study data (red circles) and modelled (yellow circles) PCI-*cv* data. On the edges, examples of dimensionless mean monthly precipitation distribution and monthly patterns for the stochastic rainfall generator parameters ν and β, for the investigated domain. Types A and B belongs to typical dry-summer climates. Type C belongs to typical humid climate. Types D belongs to typical oceanic climates, with a uniform rainfall distribution. Please refer to the online version of this paper to see this figure in colour: http://dx.doi.org/10.2166/nh.2023.026.

blue circles), with MAP ranging between 0 and 2,000 mm (mainly increasing south to north), Cv(MAP) between 0.1 and 0.5 and PCI between 10 and 25 (Figure 5). Toseek completeness, the weak climate variability of the studied region is also represented in Figure 6 (middle plot, red circles) with a very narrow range of PCI and Cv(MAP).

The ν and β monthly patterns and values were derived for the 210 gridded point rainfall EU F6 WATCH data. They clearly affect the total amount, seasonality and variability of rainfall time series (MAP, PCI and Cv(MAP)). As an example, type A and B patterns in Figure 6, showed a seasonal pattern for the ν parameters which led to seasonal precipitation patterns and high PCI values. Analogously, the type D pattern in Figure 6 showed a rather uniform pattern for the ν parameters which led to a uniform precipitation pattern and low PCI value. A number of 30 ν and β monthly parameters were appropriately set to generate synthetic rainfall time series by an application of Equations (1)–(3). Their MAP, PCI and Cv(MAP) indices overlap the WATCH data domain, that is the whole temperate to dry pan-European climate conditions (Figure 6, middle plot, yellow circles).

4.3. Simulation analysis of the relation between the 'BFI', climate indices and catchment properties

Synthetic daily streamflow time series were derived by IAHCRES simulations. Generated synthetic daily rainfall time series were used as the input for the hydrological model. Values for τs and vs model parameters, in order to simulate a large set of hydro-meteorological records, were selected to be representative of a wide range of catchments properties, beyond climate features, aimed to be explored. Indication about the range of variability for τs and vs were drawn from Longobardi & Van Loon (2018), in an investigation, on a pan-European scale, where streamflow time series from the region under investigation

in this study were also modelled. Model parameters for the sub-set of Italian catchments modelled in Longobardi & Van Loon (2018) are provided in Table 3 along with the Nash–Sutcliffe Efficiency index.

Specifically for the current study, hydrological simulations were for three different values of vs (set to 0.2, 0.5, and 0.8) to account for low to high surface soil permeability, and two values for τs (set to 30 and 300 days), to account for poorly to well-drained catchments.

The role played by catchment properties, that is by the selected model parameters, is somehow easily inferable from a conceptual perspective but the simulation approach would confirm in this sense. It is in fact quite clear that, for a given precipitation input, pervious catchments (with large vs value) would deliver larger 'BFI' than impervious ones (with small vs values). Similarly, well-drained watersheds (with large ts values) represent hydrological systems with well-sustained flows, which would imply larger 'BFI' than poorly drained watersheds (with small ts values). What is instead not inferable, from a conceptual perspective, is the role of the precipitation pattern within the year (e.g. the seasonality or intra-annual variability), here described with the PCI, and the associated inter-annual variability, here described with the annual Cv(MAP) and how they interact with the model parameters that are catchment properties. From this perspective, the simulation approach was expected to indicate basic insights into this issue.

The first result is represented in Figure 6 where, at the annual scale, the baseflow versus rainfall volume scatterplots are illustrated. Differences in precipitation seasonal patterns are underlined. Among the 30 generated rainfall time series, three daily rainfall scenarios are selected and indicated as representative of a uniform (PCI = 10.18), seasonal (PCI = 12.93), and strongly seasonal (PCI = 27.26) rainfall regime. Results are illustrated for six virtual catchments. Three different levels of proportional coefficients are considered to mimic low-permeability (vs = 0.2), intermediate-permeability (vs = 0.5) and high-permeability (vs = 0.8) catchments. Additionally, for the accounted vs values, both poorly (ts = 30 days) and well-drained (ts = 300 days) systems are modelled. As expected from a conceptual point of view, there exists a relation between the baseflow and rainfall volume, which feature clearly depends on climate settings and catchment properties. It is confirmed that, for each of the rainfall regime (PCI), and for given ts values larger 'BFI' correspond to larger vs and that for given vs values, larger 'BFI' correspond to large ts (see the location of the scatterplots in the annual rainfall-'BFI' plane).

It is more strictly gained from the simulation results that, for given ts and vs, the extent of the variability of the annual baseflow volumes increase from uniform to strongly seasonal rainfall patterns. The last observation is likely explained by the increase in rainfall annual variability when moving from uniform to seasonal climate regimes.

Besides the increase of 'BFI' variability with climate seasonality, the decrease in the annual 'BFI' is another result strictly gained from the simulation approach. This peculiarity holds in particular for well-drained catchments (ts = 300 days) and for catchments with an intermediate level of permeability (vs = 0.5). Instead, for the poorly drained systems the correlation patterns between annual 'BFI' and rainfall volume does not seem to be characterized by a definite negative sign. As the insights from Figure 7 refer only to a small number of virtual catchments, the presented results need further observation for a rational explanation. Further insights about the relationship between the 'BFI' and the rainfall properties, in particular for what concerns the rainfall variability, were gained from the simulations as below illustrated.

The left panel of Figure 8 indicates that the seasonality of the climate is relatively less important than the catchment properties for what concern the 'BFI' assessment. The 'BFI' values are almost dominated by the vs parameters and almost constant for the full range of the considered PCI, with an exception for the strongly uniform climate types (small PCI values). For a given vs, long-term 'BFI' is larger for well-drained systems. The right panel of Figure 8 instead indicates that the climate

Table 3 | IAHCRES model parameters

Catchments	f (°C^{-1})	C (mm)	τw (days)	τs (days)	τq (days)	vs	NSE
Alento	0.11	88.57	10.15	66.0	0.36	0.33	0.67
Calore	0.14	339.67	51.43	60.0	0.92	0.43	0.72
Liri	0.11	299.80	62.98	102.0	2.99	0.53	0.73
Bussento Caselle	0.07	238.72	75.90	222.7	1.35	0.81	0.67
Sele Albanella	0.08	185.05	40.07	80.0	1.17	0.55	0.72

Note: 'f' the temperature modulator factor, 'C' the catchment storage index, 'τw' the catchment drying time constant, 'τs' the slow pathway time constant', 'τq' the quick pathway time constant', 'vs' the slow pathway proportional volume

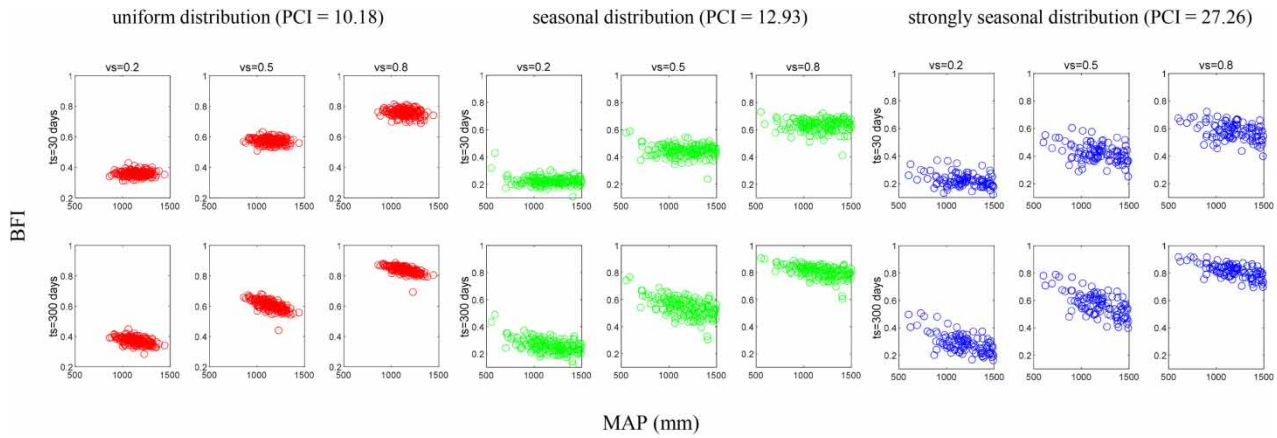

Figure 7 | Annual scale correlation between the annual 'BFI' and annual precipitation, for six virtual catchments, which differ for climate settings and model parameters.

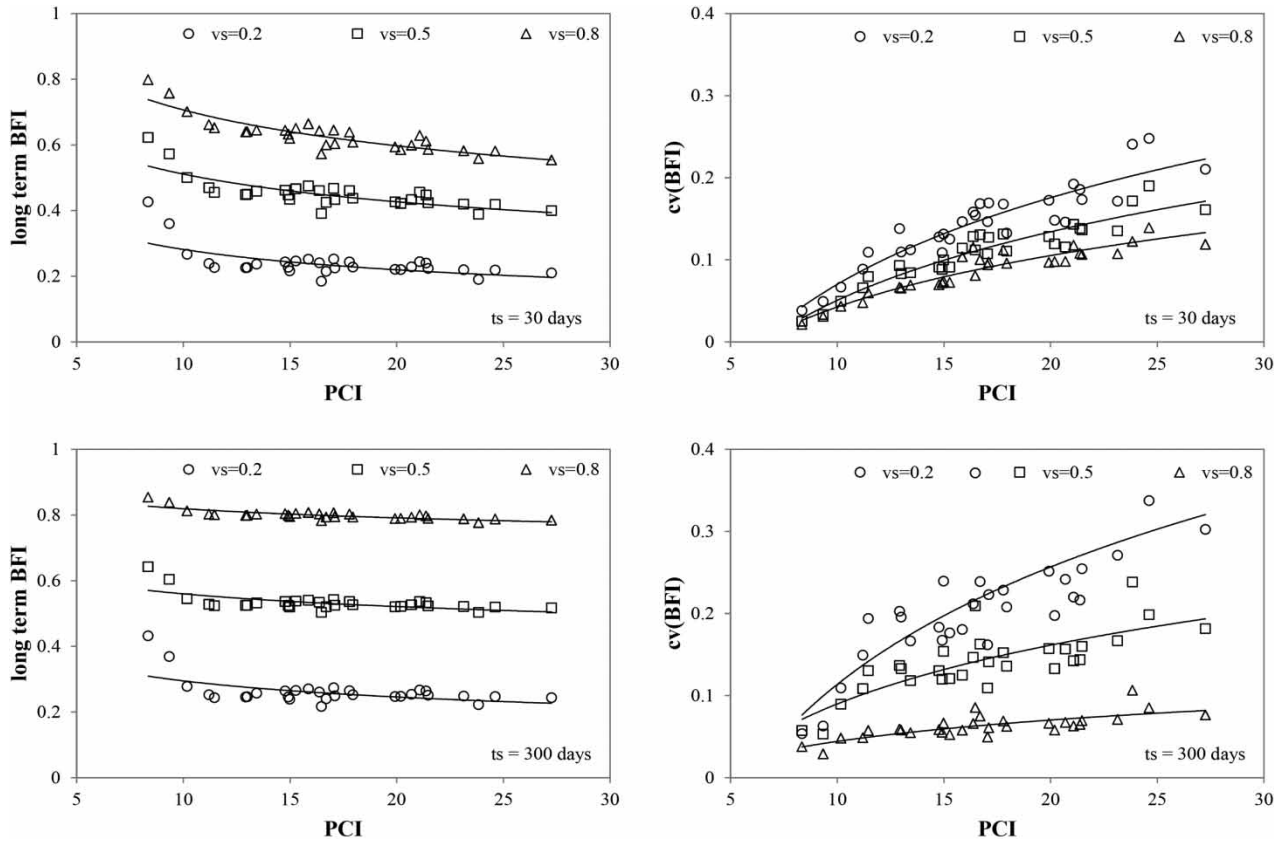

Figure 8 | The long-term 'BFI' and 'BFI' coefficient of variation dependence on the PCI, for different model parameters. (vs = 0.2, 0.5 and 0.8; ts = 30 and 300 days).

seasonality impacts the 'BFI' assessment, with large 'BFI' variability associated with large PCIs, that is with large Cv(MAP). The effect is more evident in well-drained systems.

Figure 8 provides a measure of the strength and sign of the correlation between the annual baseflow and annual rainfall, the Pearson's correlation coefficient. Pearson's correlation coefficients are plotted against a measure of rainfall variability, the

annual Cv(MAP), for different catchment properties. On a general perspective, the ρ values are consistently positive and negative respectively for poorly and well-drained catchments. To explain this feature, it is important to remember that the 'BFI' is represented by the ratio between the baseflow volume Vb and the total streamflow volume Vtot and that for each hydrological system large rainfall volumes correspond to large total streamflow volumes. In the case of well-drained systems the baseflow volume is relatively constant (persistent systems) thus an increase in rainfall only generates a significant increase in Vtot, reducing thus the ratio Vb/Vtot (negative correlation). In the case of poorly drained systems, as illustrated in the upper panel of Figure 7, the 'BFI' appears larger for lower PCI values, generally associated with large rainfall amounts. Poorly and well-drained catchments differ not only in the sign of the correlation (positive and negative respectively) but also in the fact that, in the first case, larger absolute ρ values are observed for large annual *cv* whereas, in the second case, they are observed for low annual rainfall *cv*. If as illustrated (Figure 5), small annual Cv(MAP) correspond to uniform rainfall pattern and large annual Cv(MAP) corresponds to a strong seasonal rainfall pattern. The negative correlation between precipitation and baseflow for well-drained basins is stronger in uniform climate regimes: the relationship between Cv(MAP) and MAP is strongly non-linear (Figure 6) with rainfall totals that significantly increase for the lower rainfall variability, strongly reducing the 'BFI' ratio. The decrease in 'BFI' for increasing rainfall in well-drained system is also coherent with what was found by Niu *et al.* (2017), in an Amazonian catchment where the 'BFI' value decreased for annual precipitation above the 2,500 mm threshold. In the case of poorly drained systems, the positive correlation is instead stronger in the case of large Cv(MAP). Large Cv(MAP) correspond to strongly seasonal climates which, in turn, are featured by large inter-storm periods (Longobardi & Van Loon 2018). A large inter-storm period can be comparable to the modelled delay time τs: in this case, the effect of baseflow rising produced by a rainfall shot would be rapidly drained even before the occurrence of the subsequent rainfall shot. As a result, the baseflow pattern could result in a strongly intermittent process which amounts strongly depending on the amount of rainfall at the event scale. The complex nature of the baseflow pattern for poorly drained systems is responsible for the fact that although a dominant positive correlation, Figure 9 also cases for negative correlation between Cv(MAP) and the correlation coefficient can be highlighted for the whole range of considered climate variability.

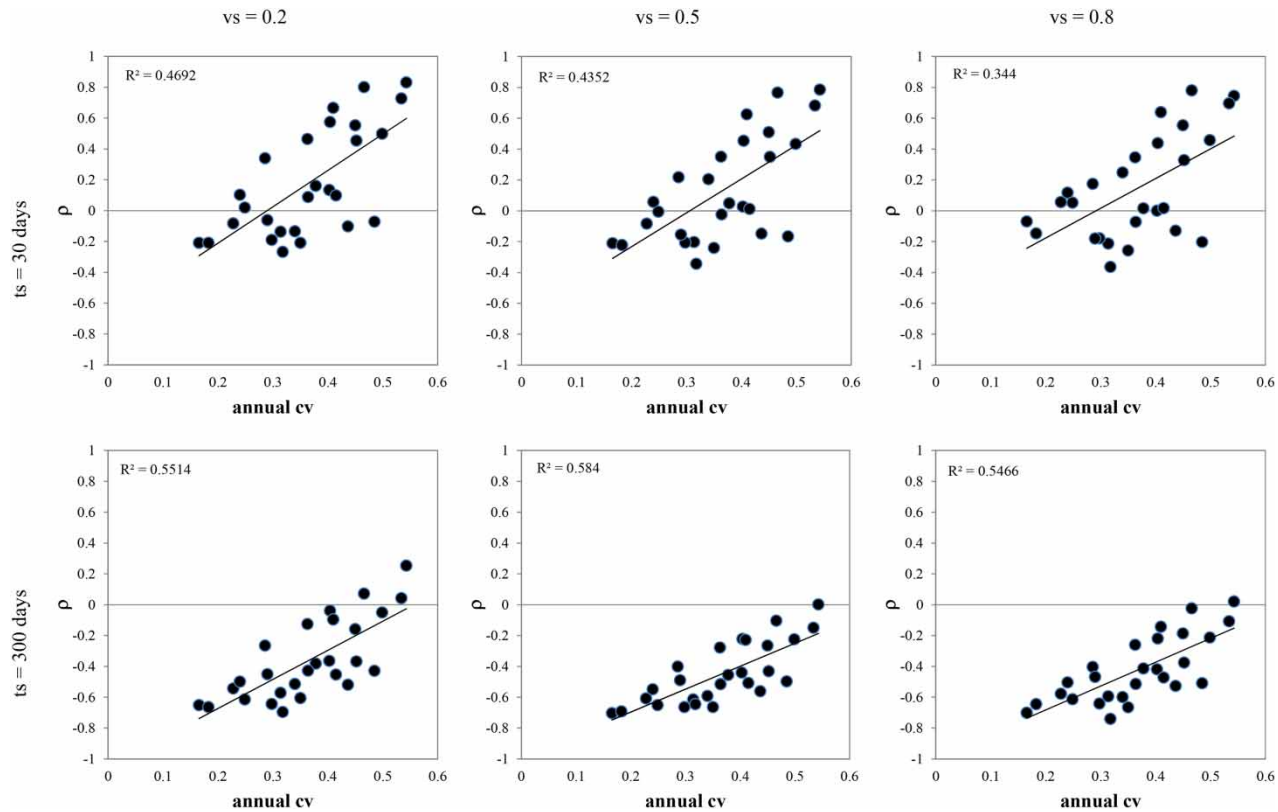

Figure 9 | Pearson's correlation coefficients between the 'BFI' and annual rainfall plotted as a function on inter-annual variability Cv(MAP), for different model parameters.

5. CONCLUSIONS AND FINAL REMARKS

This paper presented an assessment of the role of climate and catchment properties on the 'BFI'. In order to broaden the results, a coupled empirical and simulation analysis approach was adopted. In the empirical analysis, data from a Mediterranean region were analyzed to provide correlation between the 'BFI' and climate in this specific region, but the weak climate variability of the area, if considered on a very large scale, dampened the relevant findings. In the simulation analysis, rainfall scenarios were generated according to the modelling characterization given for rainfall times series provided by the WATCH data project, to describe several meteorological inputs belonging to typical temperate to dry climate domain. The IHACRES was selected to address the catchment response and synthetic total streamflow time series were processed to calculate the long-term 'BFI' and the relevant coefficient of variation Cv('BFI'). The impact of catchment properties, predictable from a conceptual perspective, was confirmed by the simulation results. The impact of other factors, such as the intra-annual and inter-annual climate variability, was only partially clear on a conceptual perspective and was inferred from the simulation approach. The following comments hold:

- Long-term 'BFI' index: the conceptual role of catchment properties was confirmed. For a given climate input large values of 'BFI' are expected for well-drained and high-permeability catchments indeed. The role played by the precipitation variability, both at the intra-annual and inter-annual scale, corresponds to a decrease in the long-term index for an increase in intra and inter-annual variability and its effect is more evident for poorly drained catchments. Poorly and well-drained catchments behave differently also with reference to the annual precipitation amount, with the 'BFI' for well-drained catchments which tends to decrease for an increase in annual precipitation.
- Cv('BFI'): as a tendency, rainfall variability propagates into 'BFI' variability, thus large Cv('BFI') are expected for large rainfall *cv* (or large PCI values). For small rainfall *cv* or PCI indices, the 'BFI' variability is comparable, independently on catchment properties. Differences arise as rainfall variability increases. Impervious watersheds, compared to previous ones, only filter a small fraction of effective rainfall through the slow pathway, the variability of total streamflow is comparable to the precipitation variability and this would entail large Cv('BFI'). The impact of the slow pathway delay time consists in large Cv('BFI') for well-drained catchments: the long recession limbs frequently intercept the effective rainfall input, increasing the 'BFI' variability contrarily to what happens for poorly drained catchments.

In a more realistic simulation experiment, it should be worth considering that the catchment response could also be affected by land use, such as considered in the empirical analysis previously reported and the nature of dominant hillslope process, which are tightly connected to climatic settings. A possible and potential solution to account for these concernments, would be the reference to a more sophisticated hydrological catchment response modelling, embedding a more detailed interaction between the soil–vegetation–atmosphere component, as well as an extension to a wider range of climatic regimes, for a more comprehensive assessment of the relative role of climate and catchment features on low-flow indices.

ACKNOWLEDGEMENTS

The authors would like to thank the anonymous referees for their encouragement and helpful comments which resulted in an improved manuscript version. The presented research results are part of the RESTORE project (PSR 2014–2020 – TIPOLOGIA 16.5.1 'Azioni congiunte per la mitigazione dei cambiamenti climatici e l'adattamento ad essi e per pratiche ambientali in corso' – Progetto RESTORE).

DATA AVAILABILITY STATEMENT

All relevant data are available from an online repository or repositories (https://www.isprambiente.gov.it/it/progetti/cartella-progetti-in-corso/acque-interne-e-marino-costiere-1/progetti-conclusi/progetto-annali).

CONFLICT OF INTEREST

The authors declare there is no conflict.

REFERENCES

Ahiablame, L., Chaubey, I., Engel, B., Cherkauer, K. & Merwadec, V. 2013 Estimation of annual baseflow at ungauged sites in Indiana USA. *Journal of Hydrology* **476**, 13–27.

Beck, H. E., van Dijk, A. I. J. M., Miralles, D. G., de Jeu, R. A. M., Bruijnzeel, L. A., McVicar, T. R. & Schellekens, J. 2013 Global patterns in base flow index and recession based on streamflow observations from 3394 catchments. *Water Resources Research* **49**, 1–21.

Benjamin, J. R. & Cornell, C. A. 1970 *Probability, Statistics and Decision for Civil Engineers*. McGraw-Hill, New York.

Botter, G., Basso, S., Rodriguez-Iturbe, I. & Rinaldo, A. 2013 Resilience of river flow regimes. *Proceedings of the National Academy of Sciences of the United States of America* **110** (32), 12925–12930.

Callegari, G., Ferrari, E., Garfì, G., Iovino, F. & Veltri, A. 2003 Impact of thinning on the water balance of a catchment in a Mediterranean environment. *The Forestry Chronicle* **79** (2), 301–306.

Daly, E. & Porporato, A. 2006 Impact of hydroclimatic fluctuations on the soil water balance. *Water Resources Research* **42**, W06401.

Fatichi, S., Ivanov, V. Y. & Caporali, E. 2012 Investigating interannual variability of precipitation at the global scale: is there a connection with seasonality? *Journal of Climate* **25** (16), 5512–5523.

Gnann, S. J., Woods, R. A. & Howden, N. J. K. 2019 Is there a baseflow budyko curve? *Water Resources Research* **55** (4), 2838–2855.

Harding, R., Best, M., Blyth, E., Hagemann, S., Kabat, P., Tallaksen, L. M., Warnaars, T., Wiberg, D., Weedon, G. P. & van Lanen, H. 2011 WATCH: Current knowledge of the terrestrial global water cycle. *Journal of Hydrometeorology* **12**, 1149–1156.

Hellwig, J., Stoelzle, M. & Stahl, K. 2021 Groundwater and baseflow drought responses to synthetic recharge stress tests. *Hydrology and Earth System Sciences* **25**, 1053–1068. https://doi.org/10.5194/hess-25-1053-2021.

Institute of Hydrology 1980 *Low Flow Studies (1–4)*. Institute of Hydrology, Wallingford, UK.

Iovino, F., Borghetti, M. & Veltri, A. 2009 Foreste e ciclo dell'acqua. *Forest@* **6**, 256–273.

Jackeman, A. J., Littlewood, I. G. & Whitehead, P. G. 1990 Computation of the instantaneous unit hydrograph and identifiable component flows with application to two small upland catchments. *Journal of Hydrology* **117**, 275–300.

Laaha, G. & Bloschl, G. 2006 A comparison of low flow regionalization methods – catchment grouping. *Journal of Hydrology*. **323**, 193–214.

Longobardi, A. & Boulariah, O. 2022 Long term regional changes in inter-annual precipitation variability in the Campania region, Southern Italy. *Theoretical and Applied Climatology* **148**, 869–879.

Longobardi, A. & Van Loon, A. F. 2018 Assessing baseflow index vulnerability to variation in dry spell length for a range of catchment and climate properties. *Hydrological Processes* **32** (16), 2496–2509.

Longobardi, A. & Villani, P. 2008 Baseflow index regionalization analysis in a Mediterranean environment and data scarcity context: role of the catchment permeability index. *Journal of Hydrology* **355**, 63–75.

Longobardi, A. & Villani, P. 2013 A statistical, parsimonious, empirical framework for regional flow duration curve shape prediction in high permeability Mediterranean region. *Journal of Hydrology* **507**, 174–185.

Lyu, S., Zhai, Y., Zhang, Y., Cheng, L., Kumar Paul, P., Song, J., Wang, Y., Huang, M., Fang, H. & Zhang, J. 2022 Baseflow signature behaviour of mountainous catchments around the North China Plain. *Journal of Hydrology* **606**, 127450.

Mehaiguene, M., Meddi, M., Longobardi, A. & Toumi, S. 2012 Low flows quantification and regionalization in North West Algeria. *Journal of Arid Environments* **87**, 67–76.

Niu, J., Shen, C., Chambers, J. Q., Melack, J. M. & Riley, W. J. 2017 Interannual variation in hydrologic budgets in an amazonian watershed with a coupled subsurface-land surface process model. *Journal of Hydrometeorology* **18** (9), 2597–2617.

Schneider, M. K., Brunner, F., Hollis, J. M. & Stamm, C. 2007 Towards a hydrological classification of European soils: preliminary test of its predictive power for the baseflow index using river discharge data. *Hydrology and Earth System Science* **11**, 1501–1513.

Sefton, C. E. M. & Howarth, S. M. 1998 Relationships between dynamic response characteristics and physical descriptors of catchments in England and Wales. *Journal of Hydrology* **211**, 1–16.

Van Dijk, A. I. J. M. 2009 Climate and terrain factors explaining streamflow response and recession in Australian catchments. *Hydrology and Earth System Science* **14**, 159–169.

Wu, J., Miao, C., Duan, Q., Lei, X., Li, X. & Li, H. 2019 Dynamics and attributions of baseflow in the semiarid loess plateau. *Journal of Geophysical Research: Atmospheres* **124** (7), 3684–3701.

Yao, L., Sankarasubramanian, A. & Wang, D. 2021 Climatic and landscape controls on long-term baseflow. *Water Resources Research* **57** (6), e2020WR029284.

First received 15 February 2022; accepted in revised form 2 December 2022. Available online 20 January 2023